Conference Paper

Direct measurement of current derivative using a delta-sigma modulator

Anuchin, A., Aliamkin, D., Shpak, D., Zharkov, A., Surnin, D. and Vagapov, Y.

This is a paper presented at the 5th IEEE International Conference on Electrical Systems for Aircraft, Railway, Ship Propulsion and Road Vehicles and International Transportation Electrification Conference (ESARS-ITEC)

Direct Measurement of the Current Derivative Using a Delta-Sigma Modulator for Sensorless Traction Motor Control

Alecksey Anuchin
Department of Electric Drives
Moscow Power Engineering Institute
Moscow, Russia
anuchin@alecksey.ru

Dmitry Aliamkin
Department of Electric Drives
Moscow Power Engineering Institute
Moscow, Russia

Dmitry Shpak
Department of Electric Drives
Moscow Power Engineering Institute
Moscow, Russia

Alexandr Zharkov
Department of Electric Drives
Moscow Power Engineering Institute
Moscow, Russia

Dimid Surnin
Department of Electric Drives
Moscow Power Engineering Institute
Moscow, Russia

Yuriy Vagapov
School of Applied Science, Computing and Engineering
Glyndwr University
Wrexham, UK
y.vagapov@glyndwr.ac.uk

***Abstract*—This paper discusses a new method of direct measurement of the current derivative applied to determine an electric motor inductance required for efficient and reliable control of sensorless AC electric drives. The method is based on the measurement of the voltage drop across a calibrated inductor implemented into the power circuit of the motor drive inverter. In order to increase accuracy and reduce transients and oscillations the measured voltage drop is processed using a delta-sigma modulator. The data stream generated by the modulator is then transferred to a microcontroller supported demodulation for further processing and filtering. The paper also presents the results of experimental investigations of three different shunt inductors. The results demonstrate a high accuracy and noise immunity of the proposed method.**

***Keywords*—current derivative, electric drive, sensorless control, delta-sigma modulator, shunt inductor**

I. INTRODUCTION

Encoderless control (or sensorless control) systems for industrial and traction AC electric drives have received much attention in the last decade. Many encoderless methods have been intensively investigated in order to design efficient and reliable selfsensing control systems for various types of electrical machines e.g. permanent magnet synchronous machine [1], [2], induction motor [3], synchronous homopolar motors [4], and switched reluctance drives [5]. All of these methods estimate the rotor position using analysis of the motor saliency ratio where the location of *d*- and *q*-axes of the machine are determined from the measurement of the motor inductance. A correct estimation of the rotor position is crucial for all types of encoderless control systems particularly operating under field-oriented [15] and direct torque algorithms.

There are several methods to measure the motor inductance for the analysis of the rotor position. One of the simplest solutions is based on a high-frequency voltage injection into the supply voltage which causes a reflection in the stator current. In the case of a round locus of the injected voltage it produces an elliptic locus of the stator current. However, a high-frequency injection results in an audible effect and torque pulsation. Another drawback of this method is the increase of the RMS and peak values of the current which results in poorer utilisation of the motor and power converter. To solve these problems, it is suggested to use a pulse-width modulation (PWM) pattern of the inverter control signal as an injection. As each PWM pattern is divided into several inverter states, these states correspond to the fixed vectors of the voltage applied to the motor windings. The response in the current behaviour under these applied voltages can be used to evaluate inductances and the rotor position [6], [7].

The evaluation of the inductances requires the measurement of current derivatives which can be obtained using the following methods:

- current measurement and evaluation of the current derivative in time [8], [9];
- current measurement and evaluation of the derivative by means of hardware differentiation [10];
- direct measurement of the current derivative [11].

The method suggested in [8], [9] processes the current curve by the least square algorithm in order to estimate the derivative. However, this method requires a large number of sequential current measurements to obtain a sufficient accuracy of the derivative estimation. As a consequence, it demands significant computational resources and the implementation of field-programmable gate array (FPGA). In [10] the current measured by the closed-loop Hall-effect sensor is processed by means of the differentiating circuit based on operational amplifiers. However, the authors [10] do not provide experimental results of its operation with a PWM driven voltage source inverter (probably due to the poor noise immunity).

A new method of the direct sensing of current derivative is suggested in [11]. This utilises the ability of a closed-loop Hall-effect sensor to transform current from primary to the secondary side. Under normal conditions the transformed current passes the measurement resistance. If an inductor is connected in series, then the voltage drop across this inductor is proportional to the current derivative in the primary winding. The major drawback of this method is the presence of the resistance component in the total voltage drop which

The research is supported by the Russian Science Foundation grant (Project № 16-19-10618).

should be taken into account and estimated under possible temperature deviations in the measurement circuit. Another problem of this method is the oscillations which occur each time when the inverter changes its state. These oscillations can be damped with an RC-snubber and require at least 10 μs to suppress them.

In order to increase the accuracy of the current derivative measurement it was suggested to use a calibrated inductor at the output of inverter. The voltage drop across the inductor is proportional to the current derivative whereas a delta-sigma modulator is used for the voltage measurement [12]. The paper discusses the implementation of this method and an analysis of its accuracy.

II. Current Derivative Measurement Circuit with Delta-Sigma Modulation

In [11] the current derivative is measured as a voltage drop across the inductor at the secondary side of the closed-loop Hall-effect sensor. High resistance of the inductor has significant impact to the measured current derivative and the obtained signal requires an additional correction. Another drawback of this approach is the oscillations of the signal during commutation of the inverter switches. In order to exclude these issues, it is suggested to implement the inductor applied for the current derivative measurement directly into the power circuits.

The voltage drop across the inductor can be measured by means of delta-sigma modulation integrated circuit (IC). Delta-sigma modulators (such as AMC1305 from Texas Instrument [13]) are currently manufactured by several companies. The IC performs modulation of the input signal and provides isolated data stream (or bitstream) transfer to the control system. Demodulation of the bitstream can be processed by an internal peripheral device of modern microcontrollers or by the programmable logic of the FPGA used for control. The schematic of the proposed solution is shown in Fig. 1.

The bitstream should be filtered with a low-pass filter. The usual choice being Sinc filters which can be of various orders. In general, the first order Sinc filter is the filter of moving average and can be represented by an IIR [14] or FIR equation, while the result of operation remains the same:

$$H_{FIR}(z) = \frac{1}{N}\left(1 + z^{-1} + z^{-2} + \ldots + z^{-(N-1)}\right), \tag{1}$$

where z is time shift operator, N represents the oversampling ratio (OSR) or the number of data stream bit used in the filter. Serial connection of the filters increases the efficient accuracy of the demodulated signal by extracting additional information carried in the switching rate of the bits [12]. Two Sinc filters connected in series form Sin2 and three filters in series form Sinc3 filter.

The input voltage of the delta-sigma modulation ICs lies in two standard ranges of ±50 or ±250 mV. Thus, the voltage drop across the shunt inductor L_{shunt} should not exceed the standard range:

$$V_{max} = L_{shunt}\frac{\mathrm{d}i}{\mathrm{d}t}. \tag{2}$$

For any given maximum phase-to-phase inductance and the inverter DC link voltage the shunt inductor value can be evaluated by the following:

$$L_{shunt} = L_{phase-to-phase\ max}\frac{V_{max}}{2V_{DC\ max}}, \tag{3}$$

where the voltage drop should be within the standard limits of $\pm V_{max}$ even under worst operational condition (when the applied DC link voltage and back-EMF of the machine are summing). Equation (2) is also used to derive the current derivative.

III. Experimental Results

A. Experimental Setup

The experimental setup shown in Fig. 2 consists of a frequency converter with diode bridge-rectifier, DC link capacitors, a three-phase inverter, and a control system based on TMS320F28335 microcontroller. Two phases of the inverter are connected to the choke with inductance of 6 mH. The control system operates under a 4 kHz control loop execution frequency and produces a sawtooth current in the choke. The sawtooth waveform of the current signal simplifies the analysis processes in the derivative measurement circuit.

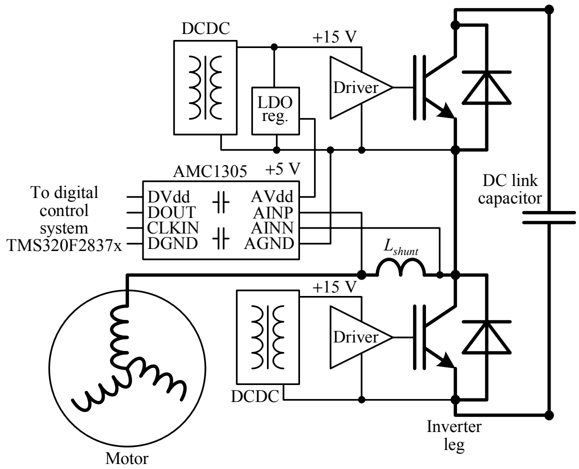

Fig. 1. Current derivative measurement topology.

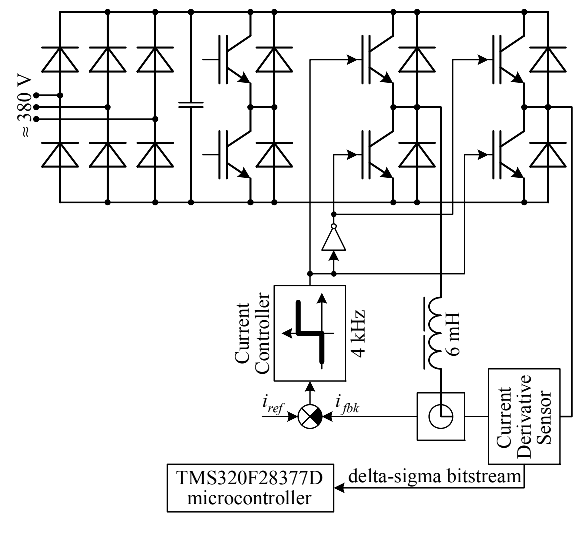

Fig. 2. Experimental setup and control system block diagram.

The current readings are taken by the control system microcontroller using an embedded closed-loop Hall-effect current sensor implemented into the frequency converter. The measurement circuit for the current derivative is connected in series to the Hall-effect sensor. It consists of a shunt inductor and a delta-sigma modulation IC installed in a separate printed circuit board (PCB) as sown in Fig. 3. The output signal from the delta-sigma modulator is a bitstream transferred to the microcontroller TMS320F28377D which supports the delta-sigma bitstream demodulation.

B. *Designs of the Shut Inductance*

The practical experiments have been conducted for the following three differing designs of the shunt inductor:

- single turn coreless coil of 25 cm long stranded wire;
- single turn of 6 cm long stranded wire with a ferrite bead;
- single turn of 6 cm long litz wire with a ferrite bead (see Fig. 3).

C. *Current Derivative Measurement*

The control system of the power converter generated the same sawtooth waveform current (shown in Fig. 4) for all of the practical experiments.

The current derivative signal was obtained using an oversampling ratio equal to 16 and Sinc3 digital filter. The results for the various designs of the shunt inductor are presented in Fig. 5.

The first experiment (Fig. 5a) shows that the resistance of the stranded wire is relatively large and could bring a significant impact to the output voltage. As the voltage is too high, and comparable with the measuring signal, its software compensation will introduce an extra error.

In the second experiment the wire was shortened to 6 cm approximately. In order to compensate for the decrease in value of the shunt inductor due to the smaller size of the coil, the wire has been equipped with a ferrite bead. The current derivative became clearly visible in the output signal waveform (Fig. 5b), however the shape of the signal indicates that the resistance of the shunt inductor is changing with time due to the skin effect.

To eliminate the skin effect, the stranded wire has been replaced with litz wire in the third experiment. Fig. 5c shows the current derivative for the shunt made of litz wire with a ferrite bead. The experimental result demonstrates that a certain impact of the shunt inductor resistance is still observed. It can be seen that a typical voltage drop is about 9.5 mV. The calculated resistance of the litz wire is 0.220 mΩ. If the peak current is 17.5 A for both positive and negative polarities, then the estimated voltage drop is

$$\Delta v = 2R_{L_{shunt}} i_{max} = 2 \cdot 0.22 \cdot 17.5 = 7.7 \text{ mV}. \qquad (4)$$

Therefore, the calculated value is less than the actual by 1.8 mV. The difference in this voltage drop can be explained by the same skin effect as in Fig. 5b. However, the difference is much smaller because only the soldered ends of the inductor are affected.

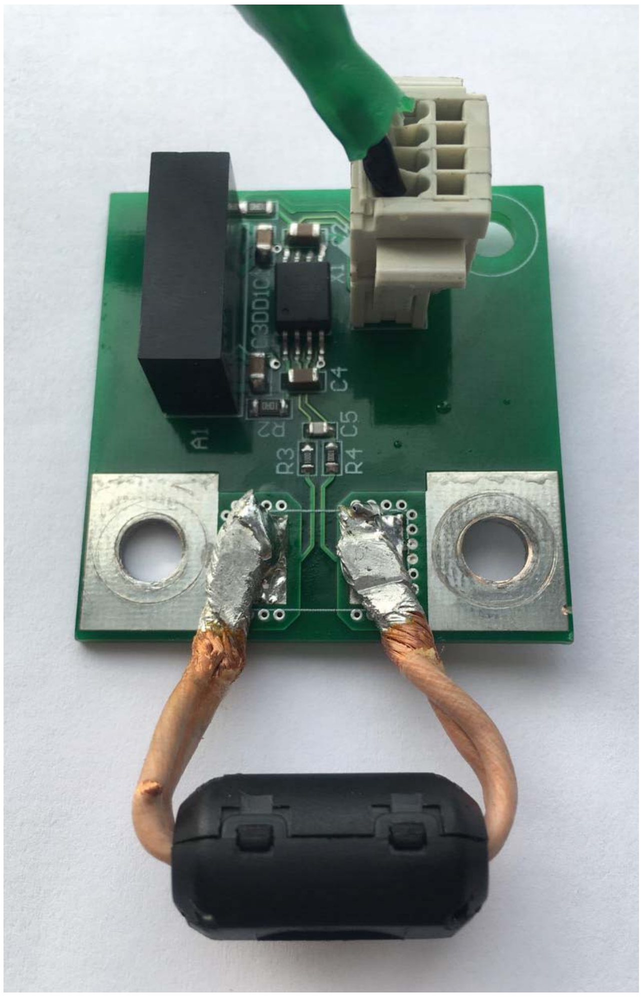

Fig. 3. Current derivative sensor.

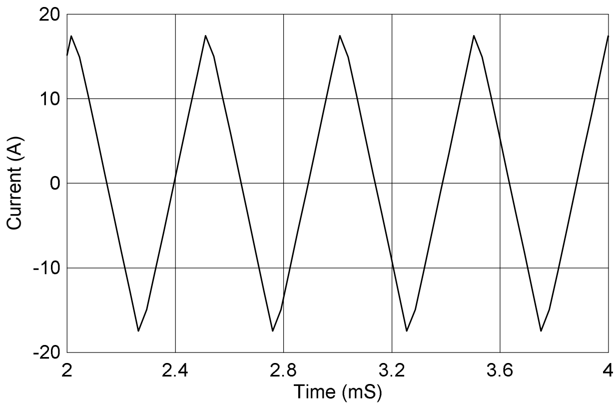

Fig. 4. Sawtooth waveform current.

The voltage drop can be reduced further by an improvement in the hardware design or by a software compensation using a computational algorithm as a function of the flowing current. As for the skin effect, it could be reduced by means of an improved design of the soldered area of the sensor PCB.

IV. Conclusions

The proposed solution provides a direct measurement of the current derivative which can be applied for encoderless motor control in industrial drives and traction applications.

The sensor has small dimensions, is cheap and provides excellent noise immunity due to the delta-sigma modulation used for the voltage drop measurement. The measured signal has no transients and oscillations which allows PWM voltage be used as an injection for the sensorless control of AC motor drives including INFORM methods [15].

However, the control system is required to provide embedded support of the sigma-delta demodulator based on a Sinc3 or similar digital filter. Further investigations will be focused on the reduction of the impact of the shunt inductor resistance and experiments with a 3-phase IPM traction motor equipped with a self-sensing position estimator.

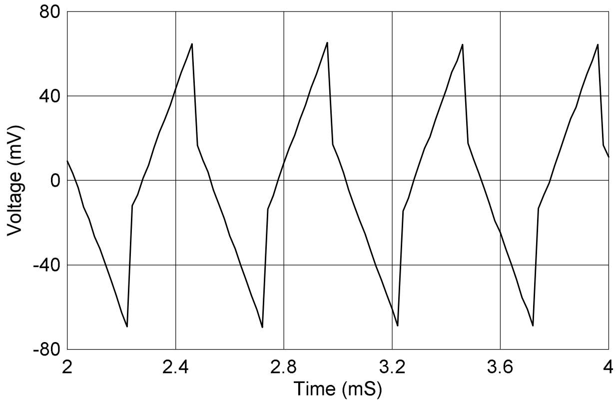

a)

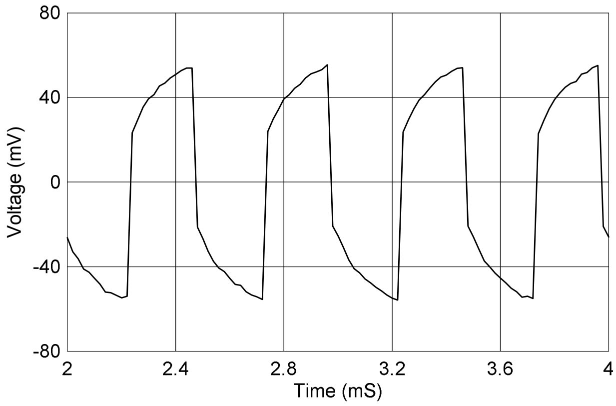

b)

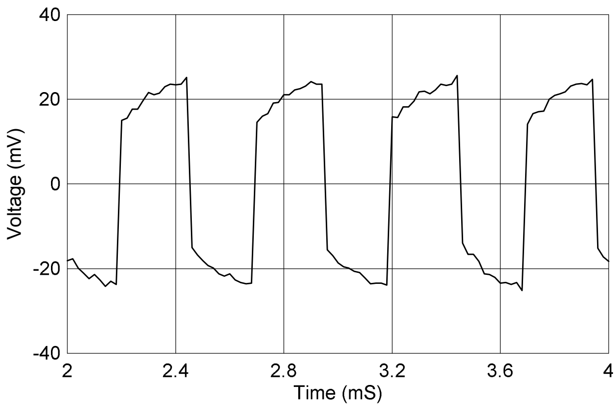

c)

Fig. 5. Current derivative signal. (a) single turn coreless coil of 25 cm long stranded wire; (b) stranded wire with a ferrite bead; (c) litz wire with a ferrite bead.

REFERENCES

[1] L. Jarzębowicz, "Sensorless IPMSM drive with rotor position estimator based on analysis of phase current derivatives," in *Proc. 2011 IEEE Int. Symp. on Industrial Electronics*, Gdansk, Poland, 27-30 June 2011, pp. 733-738.

[2] G. Foo, Z. Xinan, D.L. Maskell, and D.M. Vilathgamuwa, "Sensorless direct torque control of interior permanent magnet synchronous motor drives using the current derivative approach," in *Proc. 2015 IEEE Symp. on Sensorless Control for Electrical Drives (SLED)*, Sydney, Australia, 7-8 June 2015, pp. 1-6.

[3] G. Brando, A. Dannier, A. Del Pizzo, R. Rizzo, and I. Spina, "Torque derivative control in induction motor drives supplied by multilevel inverters," *IET Power Electronics*, vol. 9, no. 11, pp. 2249-2261, 2016.

[4] M. Lashkevich, A. Anuchin, D. Aliamkin, and F. Briz, "Investigation of self-sensing rotor position estimation methods for synchronous homopolar motor in traction applications," in *Proc. 43rd Annu. Conf. IEEE Industrial Electronics Society IECON-2017*, Beijing, China, 29 Oct.-1 Nov. 2017, pp. 8225-8229.

[5] D. Aliamkin, A. Anuchin, M. Lashkevich, and F. Briz, "Sensorless control of two-phase switched reluctance drive in the whole speed range," in *Proc. 42nd Annu. Conf. IEEE Industrial Electronics Society IECON-2016*, Florence, Italy, 23-26 Oct. 2016, pp. 2917-2922.

[6] M.X. Bui, D.Q. Guan, D. Xiao, and M.F. Rahman, "Sensorless control of interior permanent magnet synchronous motor based on the fundamental pulse width modulation excitation over a wide speed range," in *Proc. 19th Int. Conf. on Electrical Machines and Systems (ICEMS)*, Chiba, Japan, 13-16 Nov. 2016, pp. 1-6.

[7] Y. Hua, M. Sumner, G. Asher, and Q. Gao, "Sensorless control for a PM machine with reduced current distortion using space vector PWM excitation," in *Proc. 13th European Conf. on Power Electronics and Applications*, Barcelona, Spain, 8-10 Sept. 2009, pp. 1-10.

[8] M.X. Bui, D. Guan, D. Xiao, and M.F. Rahman, "A modified sensorless control scheme for interior permanent magnet synchronous motor over zero to rated speed range using current derivative measurements," *IEEE Trans. on Industrial Electronics*, 2018, doi: 10.1109/TIE.2018.2823663.

[9] Y. Duan, and M. Sumner, "A novel current derivative measurement using recursive least square algorithms for sensorless control of permanent magnet synchronous machine," in *Proc. 7th Int. Power Electronics and Motion Control Conf.*, Harbin, China, 2-5 June 2012, vol. 2, pp. 1193-1200.

[10] C. Liu, H. Yi, J.-G. Liu, and Q. Zhang, "A novel method for measuring current derivative signal with closed loop Hall-effect current sensor," in *Proc. Int. Conf. for Power Electronics, Intelligent Motion, Renewable Energy and Energy Management PCIM Europe 2015*, Nuremberg, Germany, 19-20 May 2015, pp. 1-8.

[11] A. Anuchin, A. Zharkov, D. Shpak, D. Aliamkin, and Y. Vagapov, "Current derivative measurement using closed-loop Hall-effect current sensor," in *Proc. 9th IET Int. Conf. on Power Electronics, Machines and Drives PEMD-2018*, Liverpool, UK, 17-19 April 2018, pp. 1-5.

[12] A. Anuchin, D. Surnin, and M. Lashkevich, "Accuracy analysis of shunt current sensing by means of delta-sigma modulation in electric drives," in *Proc. 17th Int. Ural Conf. on AC Electric Drives (ACED)*, Ekaterinburg, Russia, 26-30 March 2018, pp. 1-5.

[13] *AMC1305x Small, High-Precision, Reinforced Isolated Delta-Sigma Modulators*, Texas Instruments, TX, USA, Datasheet SBAS654F, June 2014, Rev. March 2017.

[14] M. Oljaca, and T. Hendrick, "Combining the ADS1202 with an FPGA digital filter for current measurement in motor control applications," Texas Instruments, Dallas, TX, USA, Application Rep. SBAA094, June 2003.

[15] M. Schroedl, "Sensorless control of AC machines at low speed and standstill based on the INFORM method," in *Proc. 31st IEEE Annu. Meeting Industry Applications Conf. IAS 96*, San Diego, CA, USA, 6-10 Oct. 1996, vol. 1, pp. 270-277.